

The STACEE Project

René A. Ong and Corbin E. Covault

Enrico Fermi Institute, University of Chicago, Chicago, IL 60637, USA

(For the STACEE Collaboration)

To appear in Proc. Towards a Major Atmospheric Cherenkov Detector-V (Kruger Park)

Abstract

The Solar Tower Atmospheric Cherenkov Effect Experiment (STACEE) is designed to explore the gamma-ray sky between 20 and 250 GeV using the atmospheric Cherenkov technique. STACEE will use large solar heliostat mirrors to reflect Cherenkov light created in gamma-ray air showers to secondary mirrors on a central tower. The secondary mirrors image this light onto photomultiplier tube cameras that are read out by fast electronics. Here we outline the important features of the STACEE design. We present an overview of the experimental site, describe the method of heliostat selection and control, and discuss the current designs for the detector components, including the secondary mirror structures, cameras, and electronics.

1. Introduction

There is a window in the gamma-ray spectrum which has yet to be systematically explored by any telescope. Current state-of-the-art atmospheric Cherenkov telescopes have energy thresholds of 250 GeV or greater. Conversely, the EGRET experiment on the Compton Gamma Ray Observatory detects few astrophysical photons above 20 GeV. Exploring the gamma-ray window between 20 and 250 GeV is a primary goal of STACEE. A more complete discussion of the scientific motivation for exploring this window can be found elsewhere (Ong 1997).

To first order, the energy threshold of an atmospheric Cherenkov telescope is limited by night sky fluctuations and scales inversely with the square root of the telescope mirror collection area. The most straightforward way to achieve a low gamma-ray energy threshold is to use a very large mirror area. Two approaches to significantly increasing mirror area have been considered. The first is to build large (e.g. 10 m diameter) mirrors from scratch. In this way the mirrors can be custom-built for Cherenkov astronomy but the costs will be relatively high. A second approach is to make use of large mirror facilities that already exist. More than a decade ago, it was pointed out that large solar mirrors (heliostats) could be used as the primary collector in an atmospheric Cherenkov telescope (Danaher *et al.* 1982). Later, a design incorporating a secondary optic was suggested by members of our group (Tümer *et al.* 1990). In the past three years, the CELESTE (Paré 1997 and Québert 1997) and STACEE (Chantell *et al.* 1997, Covault *et al.* 1997) groups have carried out tests at solar mirror

facilities to demonstrate that low energy Cherenkov telescopes can in fact be constructed at these locations. Both experiments have been funded and are now under construction. A third experiment called GRAAL (Plaga 1997) is under development. The designs of CELESTE and STACEE are similar in many respects, but here we concentrate on the issues relevant for STACEE.

The STACEE collaboration explored the possibility of using the heliostat mirrors of the Solar Two power plant near Barstow CA, USA. Initial prototype work at the Solar Two site led to the first detection of atmospheric Cherenkov radiation at such a facility (Ong *et al.* 1996). Solar Two is currently an operating power plant, and a more favorable U.S. location is the research heliostat field of the National Solar Thermal Test Facility (NSTTF) at Sandia National Laboratories in Albuquerque NM.

The overall design of STACEE is shown in Figure 1. Cherenkov light created in gamma-ray air showers reaches the ground with a broad lateral extent ~ 250 m across. The NSTTF consists of 220 heliostat mirrors (each 37.2 m² in area). STACEE uses 48 heliostats for a total reflector surface of 1785 m². The heliostats reflect the Cherenkov light onto secondary mirrors on a central tower. Three 2 m diameter secondary mirrors viewing different parts of the heliostat field are used. Light reflected from each secondary mirror is imaged onto a photomultiplier tube (PMT) camera. Each heliostat is viewed by a single PMT.

In this paper, we describe the essential features of the STACEE design. We first discuss the NSTTF site itself. We then outline the essential hardware components of STACEE, including the:

1. heliostats,
2. secondary mirror structures,
3. cameras, and
4. electronics.

2. The Site

The NSTTF is located approximately 15 km southeast of Albuquerque at an altitude of 1700 m above sea level. The site is dry and has excellent sky clarity. Weather patterns accumulated over the last thirty years predict an average precipitation of 13.4 cm per year and a yearly average of 170 fully clear days and 111 mostly clear days (NOAA 1997). We have measured the intensity of night sky background light at the site and have found an average value of $(4.3 \pm 0.9) \times 10^{12}$ photons m⁻² sec⁻¹ sr⁻¹ over the wavelength range spanned by a typical bi-alkali PMT (300-600 nm).

The NSTTF is located at Sandia National Laboratories on Kirtland Air Force Base. The facility is fully supported and operated by the U.S. Department of Energy (DOE). As such, the DOE maintains the heliostat field, heliostat control tower, and solar tower. Heliostat repair is done as a matter of course. Since the NSTTF is a research facility and not an operating power plant, there is little potential for interference between STACEE work and solar energy research.

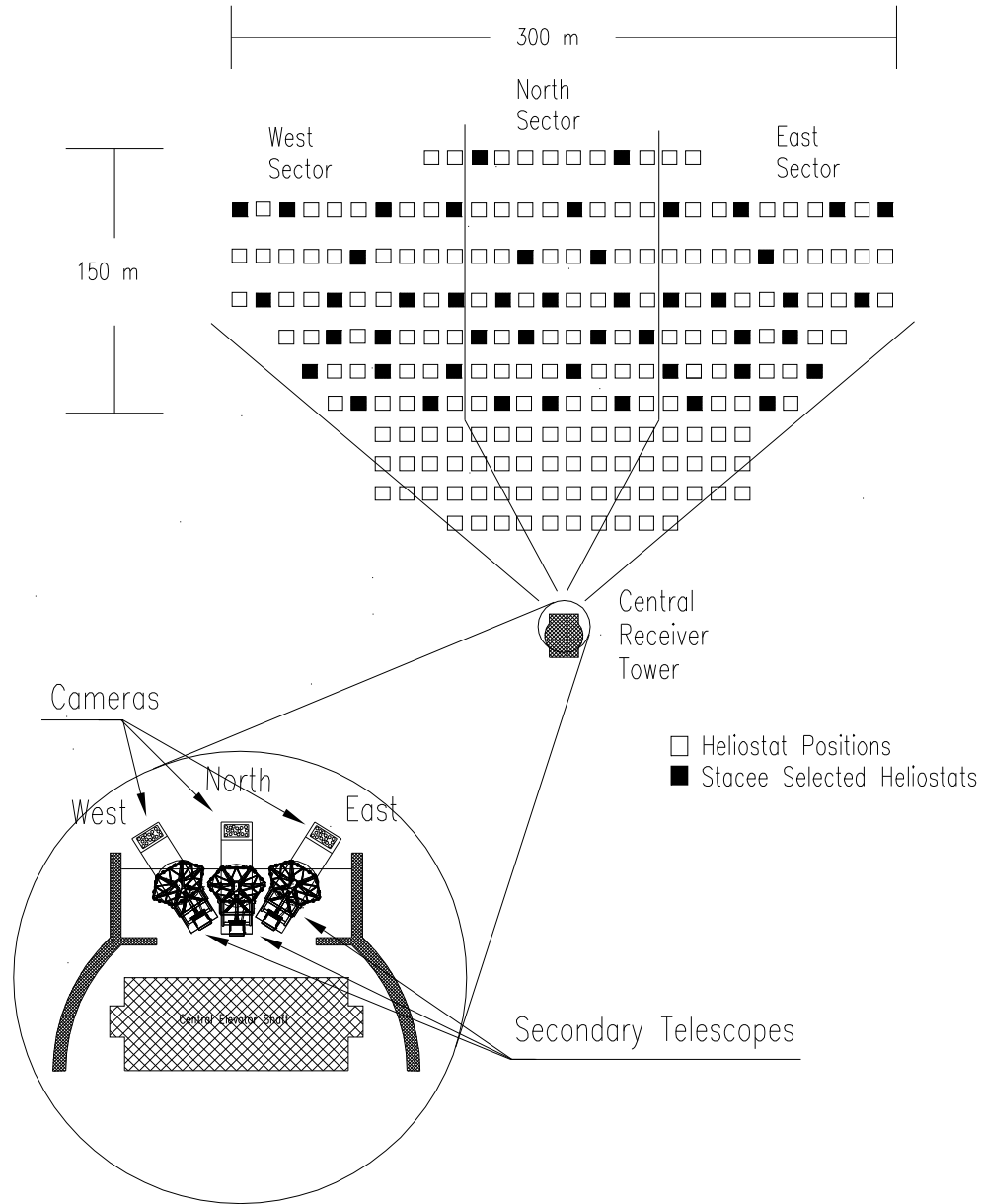


Fig. 1: Plan view of the STACEE telescope. STACEE uses 48 heliostat mirrors of the National Solar Thermal Test Facility near Albuquerque NM, USA (upper drawing). Each heliostat has an area of 37 m^2 and the distance between heliostat centers is $\sim 12.5\text{ m}$. The heliostats reflect Cherenkov radiation onto three secondary mirrors located on a central tower (lower drawing). The secondary mirrors image the light onto photomultiplier tube cameras.

We are able to schedule our observations well in advance with minimal interruption from other activities at the site.

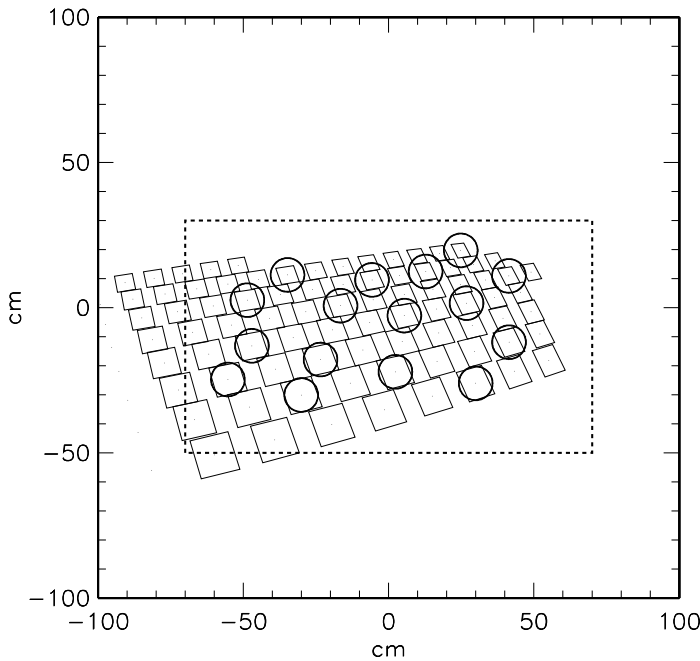


Fig. 2: View of northeastern corner of NSTTF heliostat field as seen from the position of the secondary mirror. Camera outline (rectangle) and position of PMT entrance apertures (circles) at focal plane are indicated.

3. Heliostats

Heliostat mirrors at the NSTTF consist of 25 square facets made of rear-surfaced glass. Facets for selected heliostats are aligned and focused using a television camera mounted at the top of the central tower. Each heliostat mirror can be positioned in azimuth and elevation with 13-bit precision (0.05°). The optical and pointing performance of the heliostats is found to be satisfactory for atmospheric Cherenkov astronomy and has been described elsewhere (Covault *et al.* 1997, Chantell *et al.* 1997).

3.1. Heliostat Selection

Of the 220 heliostats at the NSTTF site, we have selected 48 heliostats to be used for STACEE (16 heliostats for each of three secondary mirrors). Ideally, heliostats are selected so as to provide uniform coverage over the entire area of the field. However, selected heliostats must also not crowd each other in the focal plane of the secondary mirror. We also select heliostats to minimize off-axis aberrations. Finally, field-of-view requirements prevent consideration of heliostats that are too close to the central tower.

Figure 2 shows the view from the tower into the northeastern corner of the heliostat array corresponding to one of the three secondary mirrors. This view is imaged onto the focal plane of the mirror. The rectangular border indicates the boundary of the camera. Thick circles

indicate the position of each PMT can entrance aperture for the 16 selected heliostats in this part of the array. Note that in actual operation, non-selected heliostats will be turned edge-on and thus will not reflect light up to the secondary mirror.

3.2. Heliostat Control

All heliostats at the NSTTF are operated using a single Master Control System (MCS) based on an HP-1000 mini-computer. Software to control heliostats and to track the sun onto various targets has been previously developed by the NSTTF staff. The STACEE group has modified this software to track astrophysical sources, accounting for the fact that air showers originate near the top of the atmosphere and not at infinity. The MCS is operated directly by STACEE scientists during observations

The MCS communicates with individual heliostats over a network of serial lines. Heliostat pointing coordinates are updated at least once every 1.2 sec. Several video displays provide real-time information on every aspect of the heliostat field and warn the operator if there is a malfunction. Status and pointing information for every heliostat is logged to a file every 5 seconds.

4. Secondary Mirror Structure

A schematic view of one of the three secondary mirror structures is shown in Figure 3. The structure consists of a commercial pallet stacker which is secured to a steel base plate, or skid. The stacker raises and lowers the mirror assembly consisting of a jib-crane and spider, both made of aluminum. The jib-crane allows for azimuthal control by means of a linear actuator. The spider holds the mirror and is attached to the jib-crane by a ball joint and two actuators for elevation control. The actuators are used only for alignment and the mirror is not moved during observations.

The 2 m diameter mirror is spherical in shape and consists of seven approximately hexagonal segments, as shown in Figure 4. Each segment is a single piece of lime float glass that has been slumped, ground, polished from a 0.5" thick blank to a 2 m focal length. The glass is coated by evaporation of aluminum onto its front surface and by a protective layer of AlSiO. Each mirror segment is attached to the spider by means of a triangular aluminum base-plate which is glued to the mirror and is attached by bolts to the spider frame. Mirror adjustments are made by a three-point mounting system on each facet. The overall mirror size is set by the focal properties of the heliostats themselves. Solar images have been measured for fifteen individual heliostats and their sizes are reported in Covault *et al.* 1997. The maximum image size at the tower is 1.7 m (FWHM) and the image sizes scale as expected with the distance from the tower.

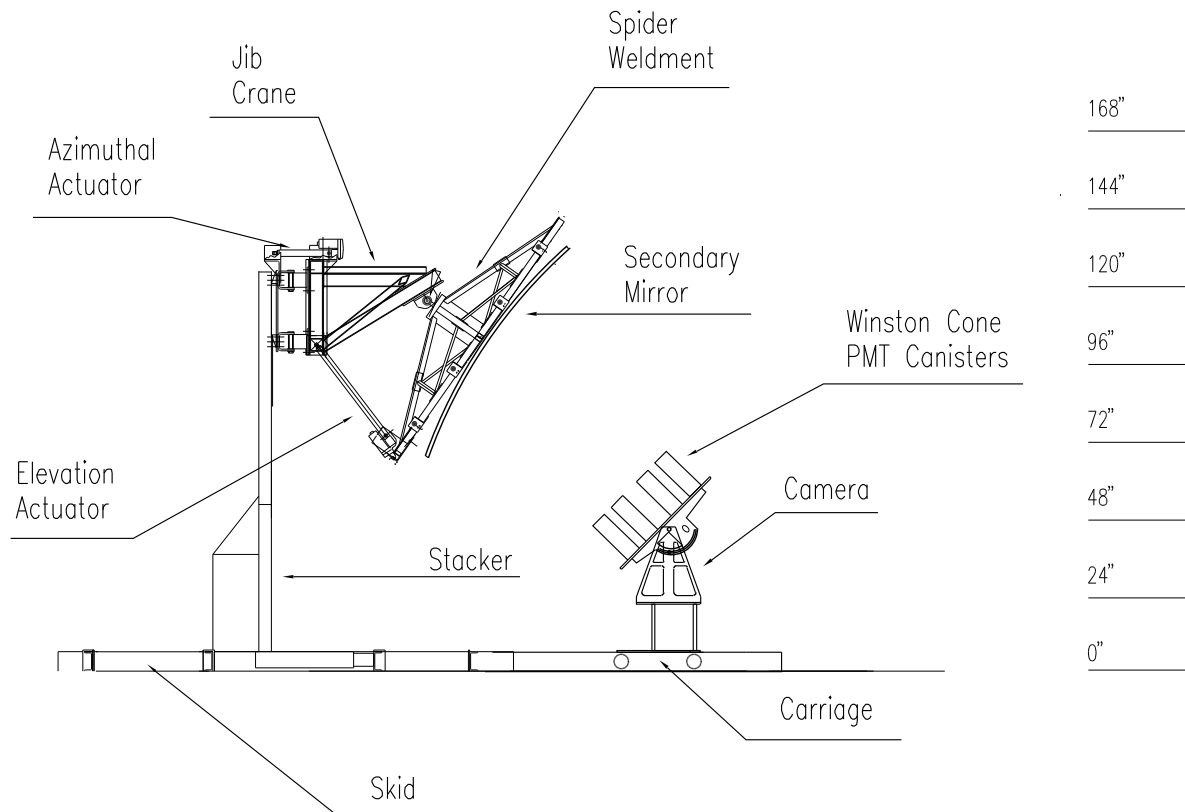


Fig. 3: Schematic diagram of the STACEE secondary mirror structure (one of three). The structure supports a 2.0 m diameter spherical mirror with a 2.0 m focal length. The mirror is positioned to reflect Cherenkov light from the heliostat field into the PMT camera. A full description of the various structure components is given in the text.

5. Camera

The camera consists of two principal components: an adjustable stand, and PMT can assemblies mounted on a slotted plate, as shown in Figure 5. The stand is a rigid structure made of aluminum bolted to a movable carriage. The carriage allows the entire camera to slide away from the tower edge to the proper focal point of the secondary mirror. The slotted plate is tilted in elevation to allow for correct focusing of the heliostat images in the center of the field-of-view of the mirror onto the entrance apertures of their respective can elements.

Each PMT can element holds an assembly which comprises an acrylic light concentrator followed by a photomultiplier tube. The PMT and concentrator are held together in a hollow metal cylinder which has an edge ring at one end and a threaded disk at the other. The disk pushes the concentrator and PMT together; they are separated by a silicone rubber cookie which provides good optical and mechanical coupling. This assembly is approximately 13 cm in diameter and 40 cm long. The concentrators are dielectric total internal reflecting concentrators (DTIRCs) (Ning *et al.* 1987).

The can elements are mounted in a sleeve arrangement. The sleeves are secured to the slotted plate with a system that allows for continuous x-y adjustment as well as canting so that

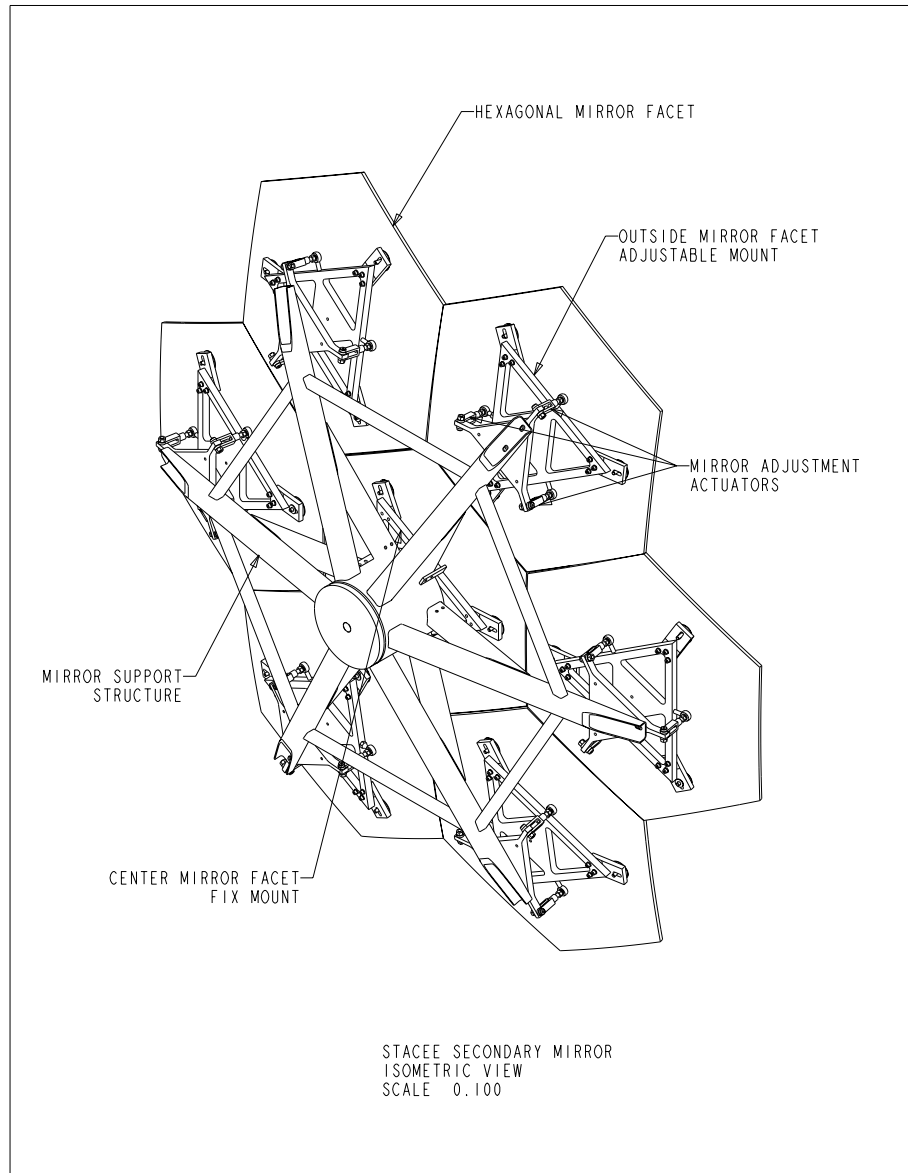


Fig. 4: Schematic diagram of a STACEE secondary mirror (one of three). The mirror has an overall width of 2 m and a 2 m focal length. It consists of seven hexagonal segments of ground, polished glass. The segments are front-surfaced with aluminum and are mounted to a rigid aluminum support structure known as the spider. Alignment of each segment is accomplished by means of a three point adjustment system, as shown.

PMTs away from the optical axis can be pointed towards the center of the mirror. For cans furthest from the optic axis of the mirror the canting angle is 17° . Operationally, one positions and cants the sleeves before sliding in the heavy PMT can elements.

The DTIRC is approximated by a converging cylinder of length between 10.6 cm and 13.2 cm. The cylinder is made of a single piece of UV transparent acrylic that has been machined on a numerically controlled mill to the proper dimensions. The front surface of the DTIRC is a sphere and the rear surface is a circular aperture. The DTIRC is designed so the field-of-view

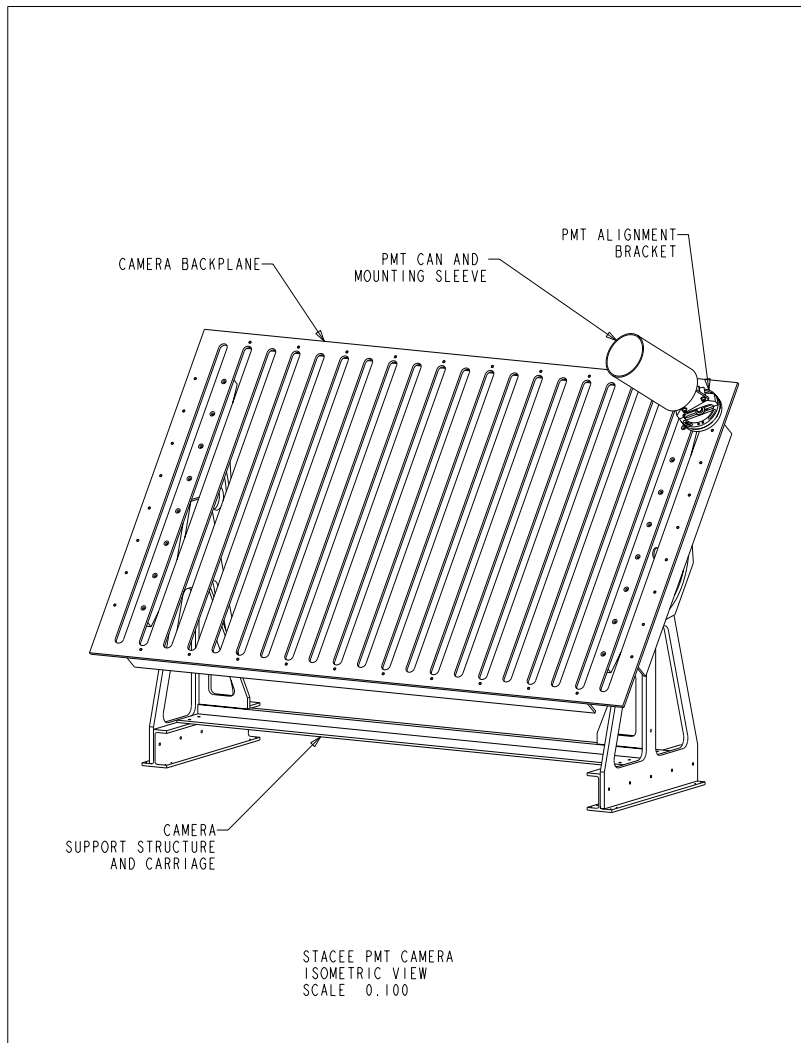


Fig. 5: Schematic diagram of a STACEE camera (one of three). The camera consists of a slotted aluminum backplane into which PMT can assemblies are mounted. Only one assembly (of sixteen) is shown for reasons of clarity. A full description of the camera is given in the text.

of each PMT is restricted. Three different types of DTIRCs are used corresponding to PMTs that view different parts of the heliostat field. PMTs viewing heliostats closest to the tower are matched with DTIRCs that have a field-of-view of 16° (half-angle), whereas PMTs viewing heliostats farthest from the tower are matched with DTIRCs having a field-of-view of 26° .

The photomultiplier tubes are chosen for high speed and moderate gain. Speed is important to minimize the level of pile-up from pulses created by night sky photons. A moderate gain is needed so that a sufficient amount of charge is generated, but at the same time the total current draw of the tube must be kept to an acceptable level ($< 100\mu\text{A}$). The PMTs (Philips XP2282) have eight dynode stages and a typical gain of $\sim 3 \times 10^5$ at a high voltage value of

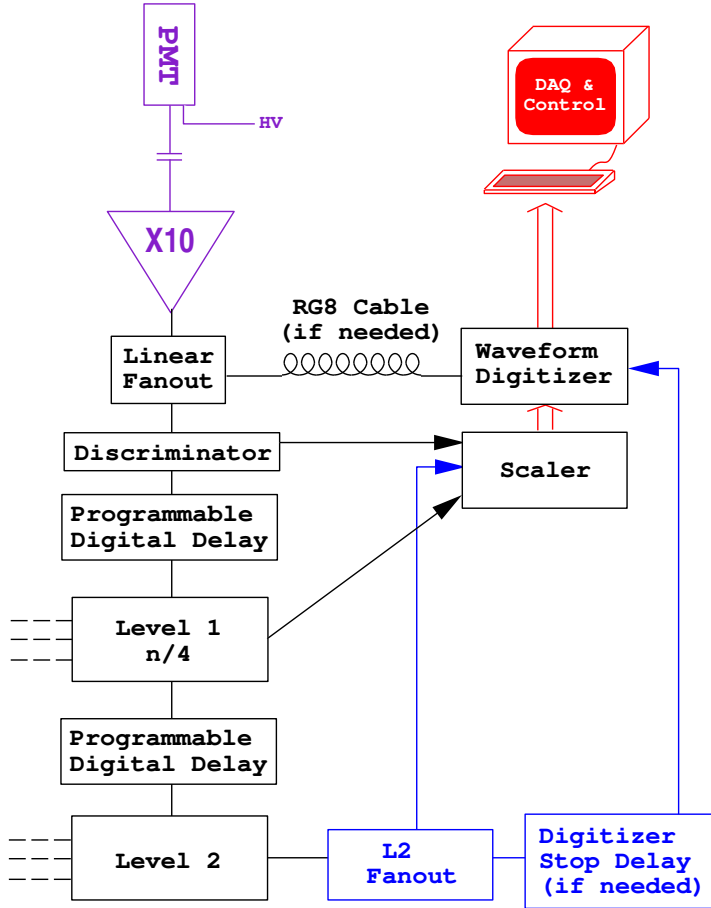


Fig. 6: Block diagram of the STACEE electronics. The PMT signals are amplified and discriminated. The discriminated signals are delayed to form a two-level (L1,L2) experiment trigger. The trigger is used to gate fast digitizers which record the PMT waveforms.

-1500 V. Each tube has a transistorized base (Philips VD 182K/C) that has been optimized for good linearity and speed. The pulse width of a single photoelectron signal at the output of the base is ~ 1.8 nsec (FWHM) and the time transit spread of the pulse is ~ 0.45 nsec. The tube has a 2" diameter bi-alkalai photocathode and a front window made of borosilicate glass.

6. Electronics

The electronics serve two major purposes. First, the PMT signals must be combined together in a coincidence circuit to form the experiment trigger. The trigger detects the occurrence of a Cherenkov air shower amidst the fluctuations of the night sky background light. Second, electronics are needed to measure the arrival time and pulse-height of the Cherenkov signal reaching each of the PMTs. The shower direction is reconstructed from the arrival time information and the pulse-height information is used to estimate the shower energy.

A block diagram of the electronics is shown in Figure 6. Commercial components are used wherever possible. The PMTs are powered by a high voltage mainframe (Lecroy 4032).

The PMT signals are capacitively coupled (time constant = 75 nsec), amplified (Phillips 776), and discriminated (Lecroy 4413). Copies of the PMT signals are generated by a linear fan-out (Phillips 748) and these copies are sampled by waveform digitizers. The waveform information is read out via Ethernet by the data acquisition (DAQ) computer.

The trigger is formed by a coincidence of the discriminated PMT signals that are delayed appropriately to bring the signals into time. The delays account for the fact that the Cherenkov light reaches different PMTs at different times because of variations in the times of flight from individual heliostats to the secondary mirror. In addition, delays are needed to account for time of flight differences due to the orientation of the shower wavefront. The trigger is composed of two distinct parts: Level 1 (L1) and Level 2 (L2)

The discriminated signals are delayed by programmable delay units (Lecroy 4518) and fixed length time of flight cables (RG 58U) and combined to form the L1 trigger. The L1 trigger consists of multiplicity logic acting on parallel groups of four PMTs (i.e. N of 4 logic). The PMTs are grouped to form L1 triggers based on the proximity of their respective heliostats. The L1 trigger signals are passed through additional programmable delay (CAEN 469) to the L2 multiplicity logic, which makes a majority decision based on the number of in-time L1 signals (i.e. N of 12 logic). The L2 trigger signifies an event trigger which stops the waveform digitizers and initiates an event read-out.

The waveform digitizers are 1 GHz sampling units with 8-bit resolution. Two commercially available products are being considered. One is a digitizer made in the VXI standard (Tektronix TVS641) and the other is a flash ADC in the VME standard (ETEP 301).

The DAQ computer will be a Silicon Graphics Workstation (Indy R4400 or equivalent). The workstation will control the CAMAC components via an Ethernet crate controller (Hytec 1365). Universal time will be recorded via a CAMAC-based Global Positioning System (GPS) clock (Hytec GPS92).

7. Conclusion

STACEE is an experiment designed to carry out gamma-ray observations in the unopened window between 20 and 250 GeV using the atmospheric Cherenkov technique. The experiment uses large heliostat mirrors of the National Solar Thermal Test Facility to achieve a very large Cherenkov photon collection area. Additional components of STACEE include secondary mirrors and structures, cameras, and electronics. The baseline design for STACEE has been finalized and the full experiment is now under construction.

Acknowledgments

STACEE is a collaboration of scientists from the University of Chicago, McGill University, the University of California (Santa Cruz), the University of California (Riverside), Barnard College, Yale University, and California State University (Los Angeles). We acknowledge the help of E. Pod, M. Houde, the engineering staff of the Yerkes Observatory, and the personnel of the McGill Physics Department machine shop. We wish to thank P. Fleury, E. Paré, J.

Québert, and D.A. Smith for many useful discussions. This work is supported in part by the National Science Foundation, the Institute of Particle Physics of Canada, the Natural Sciences and Engineering Research Council, and the California Space Institute. RAO acknowledges the support of the Grainger Foundation and the University of Chicago. CEC is a Cottrell Scholar of the Research Corporation.

References

- Chantell, M. *et al.*, Nucl Inst. Meth. Phys. Res., in press (1997).
Covault, C. *et al.*, these proceedings (1997).
Danaher, S. *et al.*, Solar Energy 28, 355 (1982).
Ning, X., Winston, R., and O’Gallagher, J., Applied Optics 26, 300 (1987).
NOAA, National Climatic Data Center, U.S. Department of Commerce, Local Climatological Data, Albuquerque NM (1997).
Ong, R.A. *et al.*, Astroparticle Phys. 5, 353 (1996).
Ong, Rene A., *Very High Energy Gamma-Ray Astronomy*, EFI 97-41, Physics Reports, submitted (1997).
Paré, E. these proceedings (1997).
Plaga, R., these proceedings (1997).
O.T. Tümer *et al.*, Nucl. Phys. B (Proc. Suppl.) 14A, 351 (1990).